

# Highly-charged ions as a basis of optical atomic clockwork of exceptional accuracy

Andrei Derevianko,<sup>1</sup> V.A. Dzuba,<sup>1,2</sup> and V. V. Flambaum<sup>2</sup>

<sup>1</sup>*Department of Physics, University of Nevada, Reno, Nevada 89557, USA*

<sup>2</sup>*School of Physics, University of New South Wales, Sydney, NSW 2052, Australia*

(Dated: August 20, 2012)

We propose a novel class of atomic clocks based on highly charged ions. We consider highly-forbidden laser-accessible transitions within the  $4f^{12}$  ground-state configurations of highly charged ions. Our evaluation of systematic effects demonstrates that these transitions may be used for building exceptionally accurate atomic clocks which may compete in accuracy with recently proposed nuclear clock.

PACS numbers: 06.30.Ft, 32.10.-f

Atomic clocks are arguably the most precise scientific instruments ever built. Their exquisite precision has enabled both foundational tests of modern physics, e.g., probing hypothetical drift of fundamental constants [1], and practical applications, such as the global positioning system. State of the art clocks carry out frequency measurements at the eighteenth decimal place [2]. As the projected fractional accuracy of such clocks is at the level of  $10^{-18}$  [3, 4], it is natural to wonder how to extend the accuracy frontier even further. We are only aware of one proposal, the nuclear clock [5], that holds the promise of reaching the improved  $10^{-19}$  accuracy level. The nuclear clock, however, relies on a yet unobserved optical transition in the radioactive  $^{229}\text{Th}$  nucleus. Here we show that the nuclear clock performances can be replicated with atomic systems, fully overcoming these challenges. We identify several highly-forbidden laser-accessible transitions in heavy stable isotopes of highly-charged ions (HCI) that may serve as clock transitions. Similarly to the singly-charged ions of modern clocks [2], HCIs can be trapped and cooled [6, 7]. The key advantage of HCIs comes from their higher ionic charge. As the ionic charge increases, the electronic cloud shrinks thereby greatly reducing couplings to detrimental external perturbations. Our analysis of various systematic effects for several HCIs demonstrates the feasibility of attaining the  $10^{-19}$  accuracy mark with existing technology.

Atomic clocks operate by locking the frequency of external oscillator (e.g., laser cavity) to a quantum (atomic/nuclear/ionic/molecular) transition. One tells time by simply counting the number of oscillations at the source and multiplying it by the known oscillation period. A suitable clock transition should have a good quality factor (Q-factor). Moreover, the clock transition frequency must remain unaffected by external perturbations. Finally, one has to be able to interrogate quantum oscillators for a long time, so the atoms should be trapped. The clock stability and accuracy generally improve with higher frequency of the clock transition,  $\nu_{\text{clock}}$ , and the current accuracy record [2] is held by singly-charged ion clocks operating at optical frequencies.

Before we start with the clock estimates, we would like to recapitulate a few basic facts about HCIs. In a multi-electron atom, optical electrons move in mean-field potential created by other electrons and the nucleus. However, as the electrons are stripped away from the atom, the field experienced by the optical electrons becomes increasingly coulombic, and one could invoke intuitive hydrogen-ion-like estimates [8]. For example, the size of the electron cloud scales with the residual nuclear (ionic) charge  $Z_i$  as  $1/Z_i$ . Since typical matrix elements are proportional to some power of atomic radius, most of the couplings to the detrimental external perturbations scale down with increasing  $Z_i$ . Higher-order responses, e. g., polarizabilities, are suppressed even further due to increasing energy intervals that scale as  $Z_i^2$ . Such suppression of couplings to external perturbations is the key to improved accuracy in the proposed HCI clock.

Trapping and cooling clock ions beneficially increases interrogation time and reduces Doppler shifts. HCIs can be loaded in ion traps [6, 7], however, due to the  $Z_i^2$  scaling of intervals most of HCIs lack low-energy electric dipole transitions that can be used for direct laser cooling. As in the state-of-the-art optical ion clocks [2], to circumvent this limitation, one may choose to employ sympathetic cooling. In this scheme, long-range elastic Coulomb collisions with continually laser-cooled  $\text{Be}^+$  ions drive HCI temperature down to mK temperatures. Heavy HCIs may be cotrapped with relatively light ions of low ionic charge, because equations of motion in ion traps depend only on the ratio of ion charge to its mass,  $Z_i/M$ . For example, Ref. [6] experimentally demonstrated sympathetic cooling of  $\text{Xe}^{44+}$  with  $\text{Be}^+$  ions. The basic idea [9] is to initially cool HCIs resistively and then load precooled HCIs into the  $\text{Be}^+$  ion trap. At sufficiently low temperatures the rates of undesirable charge-exchange processes between two ionic species become negligible. Heavier cooling species like  $\text{Mg}^+$  can be also used [2] to improve mass-matching and thereby the cooling efficiency. Additional advantage of co-trapping two ionic species comes from the possibility of carrying out quantum logic spectroscopic clock read-out [2] and initialization.

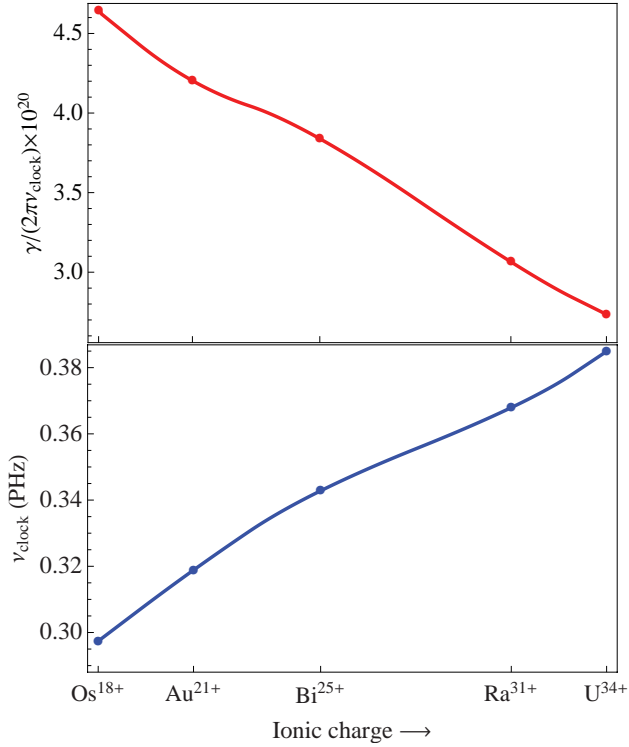


FIG. 1: Systematic trend of basic clock properties for the  $[\text{Pd}]4f^{12}$  isoelectronic sequence. Clock frequencies (lower panel) and the ratios of radiative line width to the clock frequency (upper panel) are shown as a function of ionic charge. Clock frequencies lie in laser-accessible near-infrared and optical domains, while the narrow transition width assures high quality factor.

There are many possible choices of ions. Including all degrees of ionization of the first 112 elements of the Mendeleev (periodic) table leads to 6,216 potential ions. We are interested in those ions which have closed highly-forbidden transitions in the optical frequency band. Some of the optical transitions in HCIs were identified in Refs. [10–12]. We analyzed several possibilities, and we find HCIs with the  $[\text{Pd}]4f^{12}$  ground-state electronic configuration to be especially promising for precision timekeeping.

The  $[\text{Pd}]4f^{12}$  configuration is the ground state configuration for all ions starting from  $\text{Re}^{17+}$  which have nuclear charge  $Z \geq 75$  and ionic charge  $Z_i = Z - 58$ . We computed properties of such ions using relativistic configuration interaction method described in [13, 14]; details of the calculations will be presented elsewhere. According to the Hund’s rules, in these HCIs the  $4f^{12} {}^3\text{H}_6$  and  $4f^{12} {}^3\text{F}_4$  states are the ground and the first excited states respectively. Our computed clock frequencies  $\nu_{\text{clock}}$  and ratios of radiative width  $\gamma$  to  $\nu_{\text{clock}}$  are shown in Fig. 1. The transition frequencies range from the near-infrared to the optical region and are laser-accessible. The clock states are exceptionally narrow, as the upper

TABLE I: Clock-related properties of representative HCIs of the  $[\text{Pd}]4f^{12}$  isoelectronic sequence.  $\lambda_{\text{clock}}$  is the wavelength of the clock transition,  $\tau$  is the lifetime of the upper  $4f^{12} {}^3\text{F}_4$  clock level, and  $Q$  is the quality factor. Systematic clock shifts are governed by differential static electric-dipole polarizability  $\Delta\alpha^{E1}(0)$ , black-body coefficient  $\beta_{\text{BBR}}$  and quadrupole moments of the clock states  $Q^e$ . Hyperfine structure of the clock levels is determined by the nuclear spin  $I$  and hyperfine structure constants  $A$ . Numbers in square brackets represent powers of 10.

	$^{189}\text{Os}^{18+}$	$^{209}\text{Bi}^{25+}$	$^{235}\text{U}^{34+}$
$\lambda_{\text{clock}}$ , nm	1010	874	779
$\tau$ , hrs	3.2	3.4	4.2
$1/Q$	4.6[-20]	3.8[-20]	2.7[-20]
$\Delta\alpha^{E1}(0)$ , $a_0^3$	-2.3[-3]	-2.3[-4]	-8[-5]
$\beta_{\text{BBR}}$	6.6[-20]	5.8[-21]	1.8[-21]
$Q^e({}^3\text{H}_6)$ , $ e a_0^2$	1.84[-1]	1.24[-1]	8.3[-2]
$Q^e({}^3\text{F}_4)$ , $ e a_0^2$	-1.51[-2]	-1.24[-2]	-8.4[-3]
$I$	3/2	9/2	7/2
$A({}^3\text{H}_6)$ , MHz	688	2523	-484
$A({}^3\text{F}_4)$ , MHz	719	2584	-493

clock state may decay only via highly-suppressed electric-quadrupole (E2) transition. The resulting lifetime of a few hours leads to the prerequisite high Q-factor of the clock transition, so that  $\gamma/(2\pi\nu_{\text{clock}})$  remains below the  $10^{-19}$  accuracy goal.

Clock-related properties of several representative HCIs are compiled in Table I. As an example, below we focus on  $^{209}\text{Bi}^{25+}$  ion. It has the highest transition frequency and Q-factor among stable isotopes. Being the heaviest among such isotopes has additional advantages as its large mass suppresses systematic effects related to Doppler shifts (see below).

$^{209}\text{Bi}$  has the nuclear spin of  $I = 9/2$  and, as sketched in Fig. 2, the electronic states are split into a multitude of hyperfine components. The clock transitions must be insensitive to external perturbations, such as magnetic and electric fields. Because of that we choose specific hyperfine states and magnetic substates:  $|F = 17/2, M_F = \pm 5/2\rangle \leftrightarrow |F = 13/2, M_F = \pm 9/2\rangle$  for clock transition. Similar to the virtual transition technique demonstrated in  $\text{Hg}^+$  clocks [1], the HCI clock operates on two transitions that have opposite g-factors. Averaging over the two transition frequencies eliminates the linear Zeeman shift, making clock insensitive to B-fields. While such a technique could be applied to multiple transitions, as shown below, we further required that our specific choice minimizes couplings to electric field gradients.

Clock accuracy is affected by multiple systematic effects: magnetic fields, electric fields, Doppler (motion-induced) effects, blackbody radiation (BBR), and gravity. We show that all these effects are suppressed at the desired  $10^{-19}$  fractional accuracy.

We start with examining the BBR shifts; these arise

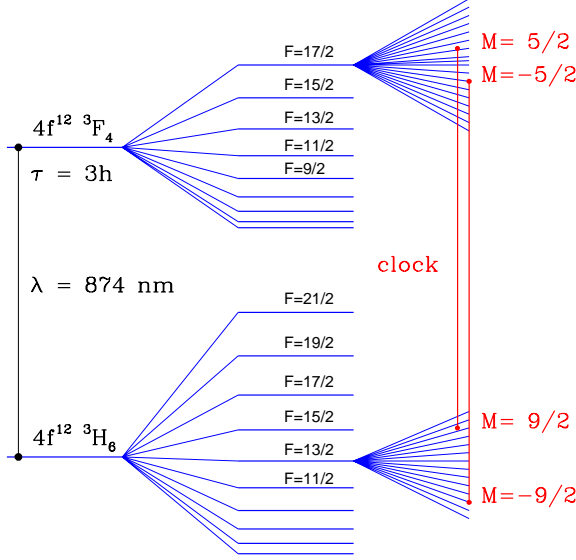


FIG. 2: Proposed virtual clock transitions in  $^{209}\text{Bi}^{25+}$  highly-charged ion. Averaging over the two indicated transition frequencies removes the first-order Zeeman shift. Specific choice of hyperfine components and magnetic sub-states minimizes shifts due to couplings to gradients of the trapping electric field.

due to perturbations by the photon bath at room temperature. The fractional shift reads [15]

$$\frac{\Delta\nu_{\text{BBR}}}{\nu_{\text{clock}}} \approx -\frac{\pi^2}{15c^3\hbar^4} \frac{(k_B T)^4}{\nu_{\text{clock}}} \Delta\alpha(0) \equiv \beta_{\text{BBR}} \times \left(\frac{T}{300 \text{ K}}\right)^4,$$

where  $\Delta\alpha(0)$  is the differential static polarizability of the clock transition and  $T$  is the BBR temperature. For HCIs, polarizabilities are suppressed as  $1/Z_i^4$  and our calculation yields  $\Delta\alpha(0) \approx -2.3 \times 10^{-4} a_0^3$  ( $a_0$  is the Bohr radius). This tiny  $\Delta\alpha(0)$  translates into the fractional BBR shift at room temperature of just  $5.8 \times 10^{-21}$ . Similarly, differential polarizability determines sensitivity to stray electric fields:  $\Delta\nu/\nu_{\text{clock}} = -\Delta\alpha(0)\mathcal{E}^2/(2\hbar\nu_{\text{clock}})$ . Typical E-fields of 10 V/m lead to negligible  $10^{-284}$ -level shifts. Cooling lasers shining on the coolant ion will lead to AC Stark shifts of the HCI clock levels. Again compared to the singly-charged ion clocks these shifts will be strongly suppressed due to much smaller  $\Delta\alpha$  and also because the HCI and the coolant ion are repelled by stronger Coulomb forces reducing the overlap of the cooling laser beam with the HCI.

The clock ion is trapped in a non-uniform field; the gradient of this field couples to the quadrupole moment  $Q$  of the clock states [16]. The quadrupole shift (QS) of

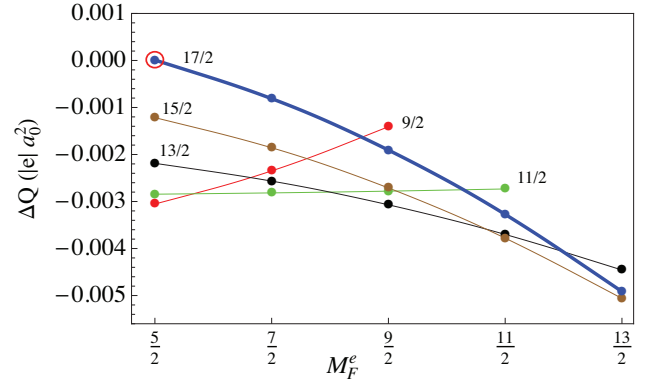


FIG. 3: Differential quadrupole moment  $\Delta Q$  as a function of magnetic quantum number of the excited clock level for  $^{209}\text{Bi}^{25+}$ . Different curves are labeled by values of the total angular momentum of the excited state  $F$ . The ground state hyperfine component remains fixed  $|F_g = 13/2, M_g = 9/2\rangle$ . The minimal value of  $\Delta Q$  is encircled; it is attained for the  $|F_e = 17/2, M_e = \pm 5/2\rangle$  “magic” state.

the clock transition is given by

$$\frac{\Delta\nu_{QS}}{\nu_{\text{clock}}} = -\frac{1}{2\hbar\nu_{\text{clock}}} \Delta Q \frac{\partial \mathcal{E}_z}{\partial z}, \quad (1)$$

where  $\Delta Q \equiv \langle Q_0 \rangle_e - \langle Q_0 \rangle_g$  is the difference in expectation values of the zeroth component of the quadrupolar tensor for the upper and lower clock states.

The relevant clock shifts for singly-charged ion clocks are sizable and considerable efforts have been devoted to mitigating this effect [1, 16]. While for the HCIs one expects  $1/Z_i^2$  suppression of  $Q$ -moments, we find that the relevant clock shifts can be still appreciable. Below we minimize the quadrupole shift by exploiting the richness of the hyperfine structure of the  $[\text{Pd}]4f^{12}$  HCI clock states. Indeed, the  $Q$ -moments of various hyperfine sub-states  $|\alpha J I; F M_F\rangle$  attached to electronic state  $|\alpha J\rangle$  may be conveniently expressed as a product of  $Q$ -moment of the electronic state  $Q^e(\alpha J)$  and a kinematic factor

$$\langle \alpha J I; F M_F | Q_0 | \alpha J I; F M_F \rangle = (3M_F^2 - F(F+1)) K(J, I, F) Q^e(\alpha J)$$

where  $Q^e$  are listed in Table I and the  $M_F$ -independent factor  $K(J, I, F)$  reads

$$K(J, I, F) = (-1)^{J+I+F} \frac{2F+1}{2J(2J-1)} \times \left\{ \begin{matrix} J & F & I \\ F & J & 2 \end{matrix} \right\} \left( \frac{(2J+3)!(2F-2)!}{(2F+3)!(2J-2)!} \right)^{1/2}.$$

As the gradient is fixed by trap parameters, we minimize the difference  $\langle Q_0 \rangle_e - \langle Q_0 \rangle_g$  by considering all possible pairs of hyperfine sub-states allowed by the E2 selection rules. The search for “magic” transitions depends

on the ratio of electronic Q-moments. These ratios can be determined experimentally by measuring frequencies of several hyperfine transitions in a trapped ion. In Fig. 3 we illustrate such a search based on our computed values of Q-moments for  $^{209}\text{Bi}^{25+}$ . We find that the minimal value of  $\Delta Q = -5 \times 10^{-6} |e| a_0^2$  is attained for the magnetic components  $|F_e = 17/2, M_e = \pm 5/2\rangle - |F_g = 13/2, M_g = \pm 9/2\rangle$ . These are the clock transitions indicated in Fig. 2.

The field gradient in Eq. (1) is fixed by the trap; we adopt the value from the  $\text{Be}^+/\text{Al}^+$  clock [17]:  $\partial \mathcal{E}_z / \partial z \approx 10^8 \text{ V/m}^2$ . Additional gradient on the clock HCI is exerted by the coolant ion. For typical ion separations of  $10 \mu\text{m}$  the resulting gradients are smaller than the indicated trapping field gradient. With such gradients, we find  $\Delta \nu_{QS} / \nu_{\text{clock}} \approx 5 \times 10^{-19}$ , which can be substantially reduced further. Indeed, due to rotational symmetry arguments, the QS can be fully zeroed out by averaging clock measurement over three orthogonal directions of quantizing B-field [16]. The power of this technique has been experimentally demonstrated for the  $\text{Hg}^+$  clock [1], where the QS was reduced by a factor of 200. The averaging out was not exact due to technical alignment issues. Combination of the “magic” choice of clock states with the averaging technique leads to our projected QS uncertainty of  $\Delta \nu_{QS} / \nu_{\text{clock}} = 2.5 \times 10^{-21}$ .

Clock frequencies are affected by magnetic fields. The first-order Zeeman shift can be eliminated by averaging the measurements over two virtual clock transitions indicated in Fig. 2. The dominant source of Zeeman-related uncertainties comes from AC B-fields caused by currents at the RF trap frequencies in conductors near the ion. Ideally, such fields would vanish at the trap axis, but in practice  $B_{\text{AC}}$  is always present due to geometric imperfections [1]. We adopt  $B_{\text{AC}} = 5 \times 10^{-8} \text{ T}$  measured in the  $\text{Al}^+/\text{Be}^+$  trap [1] as the typical value. The AC fields contribute to the second-order Zeeman shift. Calculations of the relevant differential magnetic-dipole polarizability  $\Delta \alpha^{\text{M1}}$  are dominated by intermediate states of clock hyperfine manifolds. For our choice of magnetic substates for  $^{209}\text{Bi}^{25+}$ , we find  $\Delta \alpha^{\text{M1}} \approx -2.1 \times 10^{10} \text{ Hz/T}^2$  which translates into a fractional clock shift of  $4 \times 10^{-20}$ ; it is below the sought accuracy goal.

Working with HCI requires relatively high vacuum attainable in cryogenic traps cooled with liquid helium. In the context of ion clocks, such traps were demonstrated for  $\text{Hg}^+$  ion [1]. The rate coefficient [18] for charge-exchange collisions of heavy HCIs with residual He atoms scales as  $Z_i$ :  $k \approx 0.5 \times 10^{-9} Z_i \text{ cm}^3/\text{s}$ . If the HCI were to survive for an hour, the number density of He atoms would have to be limited by  $2 \times 10^4 \text{ cm}^{-3}$ .

The zero-point-energy motion of trapped ion has a profound effect on the clock accuracy via the effect of special relativity, time dilation [19]. The fractional effect of time dilation may be evaluated as the ratio of the ion kinetic

energy  $K$  to its rest mass energy,

$$\delta \nu_{\text{TD}} / \nu_{\text{clock}} = -K / M c^2. \quad (2)$$

To estimate the effects of time-dilation, we adopt trap parameters from the ion clock of Ref. [4] based on a pair of  $\text{Al}^+/\text{Be}^+$  ions. Indeed, once the trapping fields are specified, ion motion is entirely characterized by the ratio of ionic charge to its mass,  $Z_i/A$ , where  $A$  is the atomic weight. For all the enumerated highly-charged clock ions, this ratio is about 0.15 which is comparable to the  $Z_i/A$ -ratio for  $\text{Be}^+$ . Since the trapping parameters are similar, the value of kinetic energy remains roughly the same as in the  $\text{Al}^+/\text{Be}^+$  clock, while the enumerated HCIs are about 10 times heavier than Al. This mass difference leads to suppression of the time-dilation effects with heavy HCIs, see Eq.(2). In the demonstrated  $^{27}\text{Al}^+$  clocks the uncertainties due to time-dilation are at the level of a few parts in  $10^{-18}$  with the goal of reaching the  $10^{-18}$  accuracy milestone. Due to the mass scaling argument we anticipate that  $10^{-19}$  is the plausible accuracy goal for the proposed HCI clocks. Notice that this limitation is not fundamental as it relates to the technical ability to control stray electric fields in the trap.

The clocks are affected by the effects of general relativity as well [19]. The fractional frequency difference between two clocks at differing heights on Earth’s surface is  $\Delta \nu_G / \nu_{\text{clock}} = g \Delta h / c^2$ , where  $g$  is the gravitational acceleration and  $\Delta h$  is the difference in clock height positioning. If the two identical clocks differ in height by 1 mm, the clock would acquire a  $1 \times 10^{-19}$  fractional frequency shift. Such uncertainty would limit accuracy of time transfer.

To summarize, we have shown that the highly-charged ions may serve as a basis of optical atomic clockwork at the  $10^{-19}$  fractional accuracy. Such accuracy results from the smallness of electronic cloud in ions and therefore suppressed couplings to external perturbations. The  $10^{-19}$  fractional accuracy is matched only by the proposed nuclear clock [5]; our proposed clock avoids complications of radioactivity and uncertainties in transition frequencies associated with the nuclear clock.

We would like to thank P. Beiersdorfer, T. Rosenband, E. Peik, J. Weinstein, and D. Wineland for discussions. The work was supported in part by the U.S. National Science Foundation and by the Australian Research Council.

- 
- [1] T. Rosenband, D. B. Hume, P. O. Schmidt, C. W. Chou, A. Brusch, L. Lorini, W. H. Oskay, R. E. Drullinger, T. M. Fortier, J. E. Stalnaker, S. A. Diddams, W. C. Swann, N. R. Newbury, W. M. Itano, D. J. Wineland, and J. C. Bergquist. *Science* **319**, 1808 (2008)
  - [2] C. W. Chou, D. B. Hume, J. C. J. Koelemeij, D. J. Wineland, and T. Rosenband. *Phys. Rev. Lett.* **104**, 70802 (2010)

- [3] A. Derevianko and H. Katori. *Rev. Mod. Phys.* **83**, 331 (2011)
- [4] T. Rosenband, P. O. Schmidt, D. B. Hume, W. M. Itano, T. M. Fortier, J. E. Stalnaker, K. Kim, S. A. Diddams, J. C. J. Koelemeij, J. C. Bergquist, and D. J. Wineland. *Phys. Rev. Lett.* **98**, 220801 (2007)
- [5] C. J. Campbell, A. G. Radnaev, A. Kuzmich, V. A. Dzuba, V. V. Flambaum, and A. Derevianko. *Phys. Rev. Lett.* **108**, 120802 (2012)
- [6] L. Gruber, J. P. Holder, and D. Schneider. *Phys. Scr.* **71**, 60 (2006)
- [7] M. Hobein, A. Solders, M. Suhonen, Y. Liu, and R. Schuch. *Phys. Rev. Lett.* **106**, 13002 (2011)
- [8] J. D. Gillaspay. *J. Phys. B* **34**, R93 (2001)
- [9] D. A. Church, D. Schneider, J. Steiger, B. R. Beck, J. P. Holder, G. Weinberg, L. Gruber, D. P. Moehs, and J. McDonald. *Phys. Scr.* **T80**, 148 (1999)
- [10] J. C. Berengut, V. A. Dzuba, and V. V. Flambaum. *Phys. Rev. Lett.* **105**, 120801 (2010)
- [11] J. C. Berengut, V. A. Dzuba, V. V. Flambaum, and A. Ong. *Phys. Rev. Lett.* **106**, 210802 (2011)
- [12] J. C. Berengut, V. A. Dzuba, V. V. Flambaum, and A. Ong. *arXiv:1206.0534* (2012). 1206.0534
- [13] V. A. Dzuba and V. V. Flambaum. *Phys. Rev. A* **77**, 12514 (2008)
- [14] V. A. Dzuba and V. V. Flambaum. *Phys. Rev. A* **77**, 12515 (2008)
- [15] S. G. Porsev and A. Derevianko. *Phys. Rev. A* **74**, 20502 (2006)
- [16] W. Itano. *J. Res. NIST* **105**, 829 (2000)
- [17] T. Rosenband (private communication)
- [18] G. Ferland, K. Korista, D. Verner, and A. Dalgarno. *Astrophys. J.* **481**, L115 (1997)
- [19] C. W. Chou, D. B. Hume, T. Rosenband, and D. J. Wineland. *Science* **329**, 1630 (2010)